Two-Dimensional Micro-Optics of Surface Plasmons

Sergey I. Bozhevolnyi[1,*] and Fedor A. Pudonin[2]
[1]*Institute of Physics, Aalborg University, Pontoppidanstræde 103, DK-9220 Aalborg, Denmark*
[2]*Lebedev Physical Institute, Russian Academy of Sciences, Leninskii pr. 53, Moscow, 117924 Russia*
(Received 7 November 1996)

A technique that allows one to control the elastic scattering of surface plasmon polaritons (SPP's), i.e., the SPP scattering in the surface plane, by fabricating a specially configured set of individual microscatterers is presented. Various microcomponents for two-dimensional optics of SPP's such as differently oriented micromirrors, microcavities, and a corner square micromirror, are demonstrated. SPP field distributions at single-mode microcavities exhibit spatially localized (within ~300 nm) intensity enhancement by up to ~5 times. [S0031-9007(97)02833-0]

PACS numbers: 73.20.Mf, 07.79.Fc, 42.25.Fx, 61.16.Ch

Surface plasmon polaritons (SPP's), i.e., collective oscillations of the surface electron density, can be excited along an interface between dielectric and metal in a broad spectrum of frequencies: from infrared to ultraviolet, with the only precondition being that a dielectric constant for the metal be negative [1]. Their electromagnetic fields decay exponentially into either of the neighbor media and have their maximum at the interface. For this reason, SPP's are extremely sensitive to surface properties, a circumstance that makes SPP's a useful tool for surface studies, e.g., for sensing surface contamination [2]. The development of near-field microscopy [3] has led to, among other new techniques, an exciting possibility to locally observe and investigate various SPP properties, from resonance field enhancement to localization [4].

This work has been impelled by the similarity between SPP's and waves propagating in planar (integrated optical) waveguides: Both are quasi-two-dimensional waves propagating along the surface. However, in contrast to rather sophisticated structures developed in integrated optics [5], there is very little known about possibilities for local controlling and directing SPP's, especially in the surface plane. Elastic SPP scattering, i.e., SPP scattering in the surface plane caused by surface roughness, has been studied with a scanning near-field optical microscope (SNOM), and surface structures that resembled a microcavity [6] and a microlens [7] for SPP's have been observed. It was in the course of these studies that the idea of micro-optics of SPP's as two-dimensional optics of SPP's with artificially created microcomponents has evolved [7]. Quite recently, local SPP excitation has been demonstrated by using a metal coated tapered fiber probe as a radiation source [8,9] and by changing coupling conditions (in the Kretschmann configuration) with artificial surface defects [10]. However, there have not been yet reported *artificial* surface structures that could *elastically* scatter SPP's. There are at least two serious reasons that explain such a gap in an otherwise impressive progress achieved in locally resolved studies of SPP's [4,6–10]. Since, contrary to two-dimensional guided waves in integrated optics, the maximum intensity of the SPP field is located at the surface, it is easier by far to scatter SPP's out of the surface plane than along it. In addition, the SPP propagation path is rather limited (by tens of micrometers in visible) due to the internal damping [1], a circumstance which severely limits sizes of possible optical components for SPP's and compels one to look for new approaches rather than to follow the beaten track of integrated optics.

In this Letter we propose to control the elastic SPP scattering by fabricating a specially configured set of individual microscatterers and present the appropriate technique together with first experimental observations. As far as the development of the fabrication technique is concerned, it was clear from the outset that an *elastic* microscatterer should be sufficiently large and with smooth boundaries in order to maximize the scatterer's strength while preserving an adiabatic perturbation. We believe that film material modification [9] can hardly be used for fabricating such a scatterer, as the influence of material properties on the SPP characteristics is known to be very strong [1,2]. On the other hand, some of the observed surface bumps demonstrated sufficiently effective elastic SPP scattering by exhibiting well-pronounced interference patterns related to the interference between the excited and scattered SPP's [6–9]. The technique that we suggest to use for creating deliberately similar bumps is rather simple: One has to press an uncoated fiber tip against a metal film surface. In fact, we have a suspicion that some of those bumps observed [6,7] were created during the initial approach of a fiber tip toward the surface. Once tip displacements (to and from the surface) at given surface points are controlled, a set of surface bumps that exhibits specific scattering properties can be fabricated.

The experimental setup used in this work consists of a stand-alone photon tunneling SNOM combined with a shear force based feedback system and an arrangement for SPP excitation in the usual Kretschmann configuration (Fig. 1), and is described in detail elsewhere [6]. SPP's are excited along a 45-nm-thick silver film that has been thermally evaporated on a glass prism (refractive index $n \approx 1.52$) in vacuum ($\sim 10^{-5}$ Torr) during a rather short time interval (~10 s) aiming at fabrication of

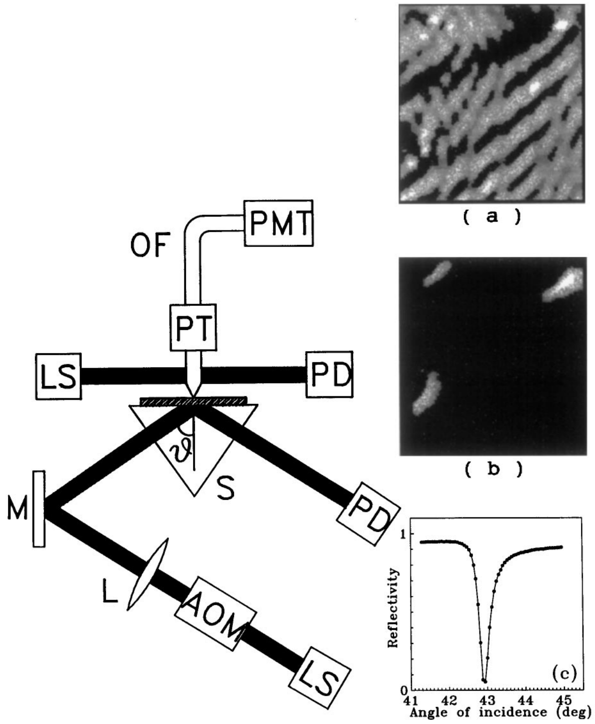

FIG. 1. Experimental setup for imaging intensity distributions of surface plasmons [(a) typical optical image of $4 \times 4.5\ \mu\text{m}^2$] simultaneously with surface topography [(b) corresponding surface image with the maximum depth of 76 nm], and for SPP excitation [(c) angular dependence of the reflected light power]. LS, laser source; AOM, acousto-optic modulator; L, lens; M, mirror; S, sample; PT, piezotranslator; OF, single-mode optical fiber; and PMT, photomultiplier tube. The polarization of light is parallel to the figure plane.

a smooth but relatively soft film. The p-polarized (electric field is parallel to the plane of incidence) light beam from a He-Ne laser ($\lambda \approx 633$ nm, $P \approx 3$ mW) is weakly focused onto the base of a prism with the silver film (focal length ≈ 500 mm, spot size $\sim 400\ \mu$m). Such an arrangement allows one to increase a local intensity of the incident beam while keeping it within the angular width of resonant SPP excitation. The reflected light is detected by a photodiode, and the SPP excitation is recognized as a minimum in the angular dependence of the reflected light power [1]. The appropriate angular dependence was measured in order to determine the resonant excitation angle [Fig. 1(c)]. By fitting the measured dependence to that calculated for the three-layer structure, the film dielectric constant ε_f and the appropriate SPP characteristics (the effective wavelength λ_{SPP} and the propagation length L_{SPP}) were determined [1]: $\varepsilon_f \approx -16 + 1.08i$, $\lambda_{\text{SPP}} \approx 612$ nm, $L_{\text{SPP}} \sim 22\ \mu$m. The SPP local field is probed with an etched (55 min in a 40% solution of hydrofluoric acid [11]) fiber tip that ensures both strong optical signal [7] and relatively faithful imaging [12]. The SPP excitation exhibited a well-pronounced resonance behavior [Fig. 1(c)] with the detected optical signal of up to 10 nW at resonance. The average optical signal was more than 20 times smaller if the incident angle was out of resonance and/or if the fiber tip was moved $\sim 1\ \mu$m away from the film surface. It means that the optical signal, which is detected with the tip-surface distance of a few nanometers (maintained with shear force feedback) and with the SPP being resonantly excited, is related to the SPP intensity distribution along the film surface [7]. Finally, it should be noted that all images presented here are oriented in the way that the excited SPP propagates from the right side toward the left in the horizontal direction.

The sample (a glass prism with the silver film) can be moved to and from a fiber tip of our stand-alone SNOM by using both the mechanical positioning system (for rough approaching with the accuracy of $\sim 1\ \mu$m) and the piezoelectric translator (for fine adjustment with the accuracy of ~ 5 nm). Since shear force feedback has a finite time constant ($\sim 1\ \mu$s, in our case), one can press a tip against a surface and, thereby, apply locally a considerable force on the film surface, simply by moving sufficiently fast the sample toward the tip. Apparently, by adjusting the speed and time of sample movement, the applied force and the resulting effect can be easily varied. It is our experience that gold and silver films evaporated thermally (in a wide range of evaporation parameters) are soft enough to be deformed with such a technique, without breaking a fiber tip. In fact, the same fiber tip has been used throughout all experiments. In these preliminary experiments, the driving voltage applied to the piezotranslator was controlled manually. Nevertheless, surface microdefects with similar scattering properties could be repeatedly produced.

It has been found that the sample displacement over 300–400 nm during ~ 1 s results in a micrometer-sized surface structure that elastically scatters the excited SPP with a noticeable efficiency. Typically, well-pronounced parabolic interference fringes were observed due to the interference of the excited SPP (with a plane phase front) and the scattered SPP (with a cylindrical phase front) [Fig. 2(d)]. Such a pattern could have been obscured by additionally present scattered SPP's, especially for a relatively weak scatterer [Fig. 2(c)]. High contrast observed normally in near-field optical images (Figs. 1–5) points to the fact that the elastic SPP scattering is rather efficient. For the same reason, shadow regions are usually seen in the lee of individual microscatterers (the shadows are especially pronounced in Figs. 2 and 3). However, it should be borne in mind that any surface defect contributes also to the inelastic SPP scattering (out of the surface plane) as well as to the nonresonance SPP excitation (in the first approximation, it is independent on the angle of beam incidence). It is only because of the aforementioned (optical) signal dependences on the excitation angle and tip-surface distance that these processes can be safely ignored in the present consideration.

Because of the axial symmetry of the fabrication process, one would expect to find circular shaped (doughnutlike) microscatterers, but that is only approximately the

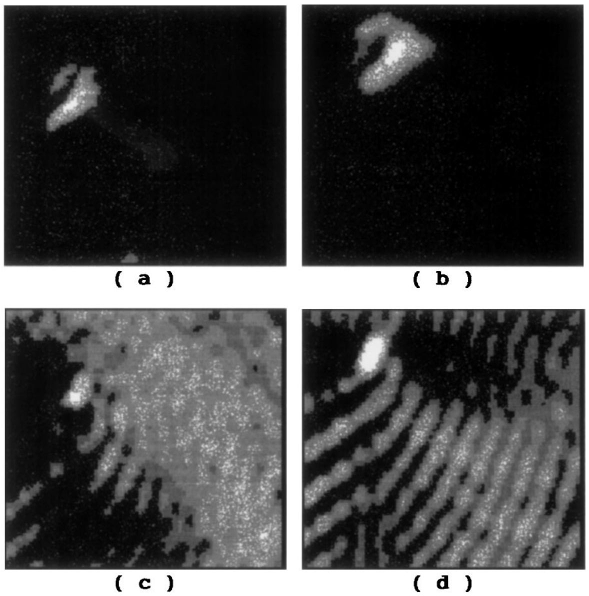

FIG. 2. Gray-scale (a), (b) topographical and (c), (d) near-field optical images (4×4 μm^2) of individual microscatterers fabricated on a 45-nm-thick silver film. Depth of the topographical images is (a) 78 nm and (b) 84 nm. Contrast, i.e., the relative difference between maximum and minimum detected optical signal, of the optical images is (c) 94% and (d) 96%.

case [Figs. 2(a) and 2(b)]. The observed asymmetry in the scatterer's shape is believed to be related to a possible asymmetry of the tip shape and to a (vertical) direction of the tip resonant oscillations (amplitude $\sim$10 nm) used in

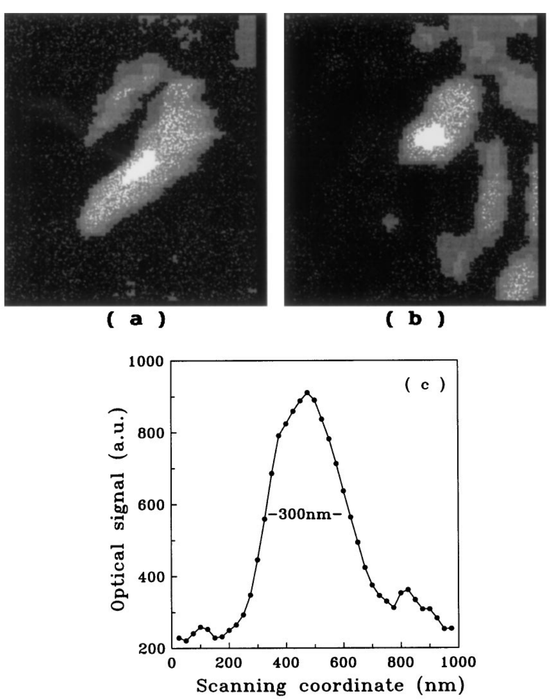

FIG. 3. Gray-scale (a) topographical, (b) near-field optical image (1.5×1.8 μm^2), and (c) partial cross section of the optical image of a single-mode microcavity. Depth of the topographical image is 82 nm. Contrast of the optical image is 98%.

shear force feedback. Since the fabricated microscatterers are sufficiently large and asymmetrical, some angular variations in the scattered SPP amplitude should be also expected, e.g., a shadow region [Fig. 2(d)] in front of a sharp corner of the microscatterer [Fig. 2(b)].

We have also noticed that most of the created microscatterers exhibited an appreciable intensity enhancement of the SPP field inside scatterer's walls [Figs. 2(c) and 2(d)]. It appears that the side walls of microscatterer produce an effect of the *single-mode* resonator (cavity) for SPP's since the separation of walls is just about half the SPP wavelength [Fig. 3(a)]. In addition, the maximum optical signal (detected inside a microresonator) exhibited the same resonance dependence on the excitation angle as the average (SPP related) optical signal. The appropriate SPP intensity distribution is of nearly ideal round shape, and exhibits the intensity enhancement by $\sim$5 times with the full width at half-maximum (FWHM) of $\sim$300 nm ($\approx \lambda_{\rm SPP}/2$) [Figs. 3(b) and 3(c)]. Such a microcavity is somewhat similar to the cavity formed by the walls of the metal coated fiber tip [9], and can also be viewed as a *SPP quantum dot* with distinct resonance properties. Dispersion of the microcavity showed up via the circumstance that the intensity enhancement was observed to vary strongly (from $\sim$1 to $\sim$5) for similar structures (Figs. 1–5).

Different optical microcomponents for SPP's can be created by fabricating specially designed arrays of microscatterers. Several microscatterers lined up with small separations would evidently produce a mirror that reflects the excited SPP in accordance with the law of reflection. The interference fringes due to the excited and reflected SPP would then be oriented parallel to the mirror line, i.e., to the line connecting microscatterers, and can be considered as a two-dimensional analog of the well-known Wiener fringes. Various differently oriented micromirrors consisting of only 2–3 scatterers were successfully fabricated (Fig. 4). Well-pronounced and properly oriented interference fringes that are seen on the presented images demonstrate convincingly the efficiency of the created micromirrors.

It is clear that once the problem of fabricating micromirrors is solved, numerous components for SPP's can be designed and produced by using a micromirror as a basic element. As an example of such a development, we present here a two-dimensional analog of a corner cube mirror, whose main property is in reflecting incident light in the exactly opposite direction (with any cube orientation). Following the concept developed above, we fabricated a corner square micromirror consisting of only three scatterers that formed a right angle triangle (Fig. 5). The appropriate near-field optical image is quite remarkable and worth considering in more detail. Notwithstanding a small image size, two regions with different kinds of interference fringes can be distinguished. Inside the triangle of microscatterers, there are two sets of interference Wiener fringes, each related to the reflection from an individual micromirror. Outside and to the right from

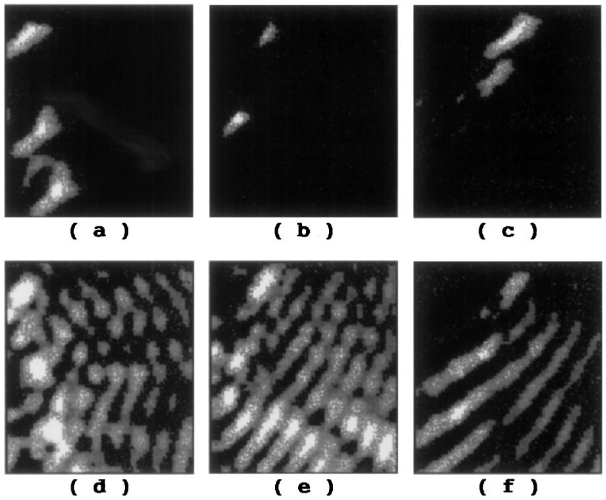

FIG. 4. Gray-scale (a), (b), (c) topographical and (d), (e), (f) near-field optical images ($2.6 \times 3\ \mu\text{m}^2$) of differently oriented micromirrors. Depth of the topographical images is (a) 99 nm, (b) 96 nm, and (c) 82 nm. Contrast of the optical images is (d), (e) 95% and (f) 88%.

the corner square micromirror, the two sets are gradually transforming into fringes corresponding to the interference between the excited and backscattered SPP's. This transformation manifests the transition from the region with single SPP scattering being dominating to the region with double SPP scattering (due to successive reflections from two micromirrors), and indicates one of possible phenomena involved in the formation of the backscattered SPP observed recently on rough silver films [7,13].

In summary, we have presented a concept of micro-optics of SPP's as two-dimensional optics of SPP's with artificially created microcomponents, which allow one to control and manipulate with elastic SPP scattering. The appropriate technique for fabricating special configurations of individual microscatterers has been presented together with the first experimental observations of differently oriented micromirrors, single-mode microcavities, and a corner square micromirror. The extension of the developed technique for producing virtually any conceivable micro-component and their combination is relatively straightforward. One can easily combine tip scanning (along the surface) with pressing it against the surface in order to fabricate linelike (straight and curved) structures (instead of doughnutlike bumps). Taking into account a large field enhancement due to the resonance SPP excitation [1], we believe that micro-optics of SPP's (with near-field microscopy as a diagnostic technique) can find many applications, e.g., in local (linear and nonlinear) spectroscopy, surface sensing, and, in general, as a tool for local studies of two-dimensional wave phenomena on the subwavelength scale. One cannot help suggesting to fabricate a micro-SPP-laser based on a single-mode microcavity, e.g., by placing a polymer microsphere doped with a dye in the center of the cavity and pumping such a structure with a metal coated fiber tip as a radiation source [8,9].

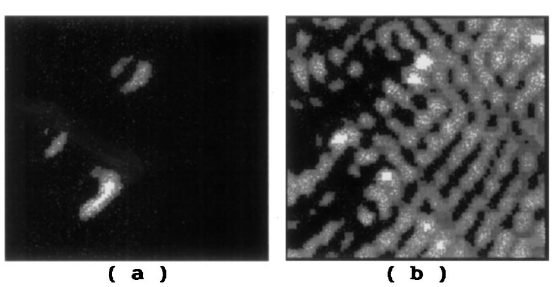

FIG. 5. Gray-scale (a) topographical and (b) near-field optical image ($4 \times 4\ \mu\text{m}^2$) of a corner square micromirror. Depth of the topographical image is 82 nm. Contrast of the optical image is 95%.

The authors thank B. Vohnsen for help and discussions. One of us (F. A. P.) gratefully acknowledges financial support from the Russian States Programmes: Surface Atomic Structures (Grant No. 95-1.19) and Physics of Solid Nanostructures (Grant No. 1-010).

*Electronic address: sergey@physics.auc.dk

[1] H. Raether, *Surface Plasmons*, Springer Tracts in Modern Physics Vol. 111 (Springer, Berlin, 1988).

[2] R. J. Bussjager and H. A. Macleod, Appl. Opt. **35**, 5044 (1996).

[3] *Near Field Optics*, edited by D. W. Pohl and D. Courjon (Kluwer, The Netherlands, 1993).

[4] M. Specht, J. D. Pedarnig, W. M. Heckl, and T. W. Hänsch, Phys. Rev. Lett. **68**, 476 (1992); O. Marti *et al.*, Opt. Commun. **96**, 225 (1993); P. Dawson, F. de Fornel, and J.-P. Goudonnet, Phys. Rev. Lett. **72**, 2927 (1994); D. P. Tsai *et al.*, Phys. Rev. Lett. **72**, 4149 (1994); R. B. G. de Hollander, N. F. van Hulst, and R. P. H. Kooyman, Ultramicroscopy **57**, 263 (1995); Y.-K. Kim *et al.*, Appl. Phys. Lett. **66**, 3407 (1995); S. I. Bozhevolnyi, B. Vohnsen, I. I. Smolyaninov, and A. V. Zayats, Opt. Commun. **117**, 417 (1995).

[5] R. G. Hunsperger, *Integrated Optics* (Springer, Berlin, 1995).

[6] S. I. Bozhevolnyi, I. I. Smolyaninov, and A. V. Zayats, Phys. Rev. B **51**, 17 916 (1995).

[7] S. I. Bozhevolnyi, Phys. Rev. B **54**, 8177 (1996).

[8] B. Hecht *et al.*, Phys. Rev. Lett. **77**, 1889 (1996).

[9] B. Hecht, D. W. Pohl, and L. Novotny, in *Optics at the Nanometer Scale*, edited by M. Nieto-Vesperinas and N. Garcia (Kluwer, The Netherlands, 1996), p. 151.

[10] I. I. Smolyaninov, D. L. Mazzoni, and C. C. Davis, Phys. Rev. Lett. **77**, 3877 (1996).

[11] S. I. Bozhevolnyi, O. Keller, and M. Xiao, Appl. Opt. **32**, 4864 (1993).

[12] S. I. Bozhevolnyi, B. Vohnsen, E. A. Bozhevolnaya, and S. Berntsen, J. Opt. Soc. Am. A **13**, 2381 (1996).

[13] S. I. Bozhevolnyi, A. V. Zayats, and B. Vohnsen, in *Optics at the Nanometer Scale*, edited by M. Nieto-Versperinas and N. Garcia (Kluwer, The Netherlands, 1996), p. 163.